

MixTrain: Scalable Training of Verifiably Robust Neural Networks

Shiqi Wang*, Yizheng Chen*, Ahmed Abdou[†] and Suman Jana*

*Columbia University

[†]Pennsylvania State University

Abstract— Making neural networks robust against adversarial inputs has resulted in an arms race between new defenses and attacks that break them. The most promising defenses, adversarially robust training and verifiably robust training, have limitations that severely restrict their practical applications. The adversarially robust training only makes the networks robust against a subclass of attackers (e.g., first-order gradient-based attacks), leaving it vulnerable to other attacks. In this paper, we reveal such weaknesses of adversarially robust networks by developing a new attack based on interval gradients. By contrast, verifiably robust training provides protection against any L-p norm-bounded attacker but incurs orders of magnitude more computational and memory overhead than adversarially robust training. Therefore, the usage of verifiably robust training has so far been restricted only to small networks.

In this paper, we propose two novel techniques, stochastic robust approximation and dynamic mixed training, to drastically improve the efficiency of verifiably robust training without sacrificing verified robustness. Our techniques leverage two critical insights: (1) instead of computing expensive sound over-approximations of robustness violations over the entire training set, sound over-approximations over randomly subsampled training data points are sufficient for efficiently guiding the robust training process. Sound over-approximation over the entire training dataset are only required for measuring the verified robustness of the final network; and (2) We observe that the test accuracy and verifiable robustness often conflict (i.e., increasing one decreases the other) during the training process after certain training epochs. Therefore, we use a dynamic loss function to adaptively balance the accuracy and verifiable robustness of a network for each epoch.

We designed and implemented our techniques as part of MixTrain and thoroughly evaluated it on six different networks trained on three popular datasets including MNIST, CIFAR, and ImageNet-200. Our detailed evaluations show that MixTrain can achieve up to 95.2% verified robust accuracy against L_∞ norm-bounded attackers while taking 15 and 3 times less training time than state-of-the-art verifiably robust training and adversarially robust training schemes, respectively. Furthermore, MixTrain easily scales to larger networks like the one trained on ImageNet-200 dataset, significantly outperforming the existing verifiably robust training methods.

I. INTRODUCTION

Neural networks have been shown to be vulnerable against carefully crafted adversarial inputs [1]. Such vulnerabilities can have potentially fatal consequences especially in security-critical systems such as autonomous vehicles [2], [3], [4] and unmanned aircrafts [5], [6], [7], [8]. Unfortunately, most of the proposed defenses provide no clear security guarantee and have been consistently broken by increasingly stronger attacks resulting in an arms race [9], [10], [11], [12], [13], [14].

So far, only two principled robust training methods (adversarially robust training and verifiably robust training) have

been found to be robust against a wide range of attacks. However, both of them suffer from significant limitations severely restricting their practical applicability. The adversarially robust training only makes the networks robust against a specific subclass of attackers (e.g., known attacks using first-order gradients), leaving it potentially vulnerable to other attacks. This is not just a hypothetical concern. In this paper, we demonstrate a new class of first-order interval gradient attacks that cause up to 40% increase in attack success rate against state-of-the-art adversarially robust networks. By contrast, verifiably robust training provides sound protections against any L-p norm-bounded attackers but incurs orders of magnitude more computational and memory overhead than adversarially robust training. Therefore, the usage of verifiably robust training so far has mostly been restricted to only small networks.

In this paper, we solve these challenges by designing MixTrain, a scalable verifiably robust training technique that can provide strong verifiable robustness against any L-p norm-bounded attacker with significantly faster training time than any existing robust (both adversarial and verifiable) training schemes. Essentially, MixTrain gives the best of both adversarially and verifiably robust training, i.e., protection against a strong attacker while still keeping the training process efficient. Below, we first summarize the main causes behind the scalability of existing verifiable robust training schemes and then describe how we address these challenges.

All robust training schemes essentially add a robustness component to the loss function that provides an estimate of robustness violations an attacker can potentially induce for the current state of the network. The robust loss (in some cases together with regular loss) is then minimized by searching for the appropriate network weights during the robust training process. The main distinguishing factor between adversarially robust and verifiably robust training is the method used to compute the robust loss during the training process. Adversarially robust training uses different existing attacks to get a lower bound on the robustness violations and therefore can only defend against a specific (or a specific class of) attack(s) even when the training process achieves low robust loss value. By contrast, verifiably robust training uses sound over-approximation methods like symbolic interval analysis [7], [15], abstract interpretation [16], [17], and robust optimization techniques [18] to find a sound upper bound on the robustness violations that can be triggered by an L-p norm-bounded attacker.

We observe that existing verifiably robust training techniques suffer from two major limitations. First, during

each training epoch (i.e., one pass over the training data), the sound over-approximation methods are run for each training data point to estimate the robustness violations given the current set of weights of the network. This is an extremely computation- and memory-intensive process. Second, the robust loss and regular loss often conflict during the robust training process, i.e., decreasing one increases the other (as shown in Section IV-A). Such conflicts prevent verifiably robust training from efficiently achieving high test accuracy.

We propose two novel techniques, stochastic robust approximation and dynamic mixed training, to address the issues mentioned above to make verifiably robust training significantly more efficient. First, we observe that sound over-approximation of robustness violations for each training data point is not necessary during training to learn a network with high verifiable robustness. Sound over-approximations of robustness violations over a randomly selected subset of the training data can still make the robust training process converge to a verifiably robust network over all the training and test data. This approach drastically cuts down the training overhead. Second, we use a dynamic loss function to adaptively balance the robust loss and regular loss for each epoch that can increase both test accuracy and verifiable robustness simultaneously.

We implemented and thoroughly evaluated MixTrain on six different neural networks trained on three popular datasets including MNIST, CIFAR, and ImageNet-200. While our techniques are generic and can integrate with any sound over-approximation method, in this paper, we used symbolic intervals [15] to soundly over-approximate the number of robustness violations. Our detailed evaluations show that MixTrain can achieve up to 95.2% verified robust accuracy against L_∞ norm-bounded attackers while taking $15\times$ and $3\times$ less training time than state-of-the-art verifiably robust training [19] and adversarially robust training schemes [20], respectively. Furthermore, MixTrain easily scales to larger networks trained on ImageNet-200 dataset and significantly outperforms earlier robust training methods. MixTrain also requires $10\times$ less memory, on average, than existing verifiably robust training schemes.

Our key contributions are summarized below:

- We present a new first-order interval gradient attack that causes up to 40% more violations in the state-of-the-art adversarially robust networks.
- We propose two novel techniques (i.e., stochastic robust approximation and dynamic mixed training) for making the verifiably robust training process highly efficient and effective at minimizing both robust loss and regular loss simultaneously.
- We implemented our techniques as part of MixTrain and thoroughly evaluated on six different networks trained on three popular datasets including MNIST, CIFAR, and ImageNet-200. MixTrain can achieve up to 95.2% verified robust accuracy against L_∞ norm-bounded attackers while taking $15\times$ and $3\times$ less training time than state-of-the-art verifiably and adversarially robust

methods, respectively.

II. BACKGROUND

In this section, we provide an overview of how robust training of Neural Networks (NNs) can be formulated as a robust optimization problem to clearly explain the challenges behind robust training. We further describe three different robustness definitions (adversarial [20], [21], distributional [21], and verifiable robustness [19], [17], [22]) that assume different threat models and summarize different existing training schemes for making NNs robust under these definitions and their limitations.

A. Robust Optimization

Robust optimization techniques broadly try to find solutions that are robust under certain bounded perturbations in different parameters of the target optimization problem. Training an NN that is robust to adversarial inputs, created by adding some bounded perturbations to benign inputs, can also be represented as a robust optimization problem. Formally, a NN $f_\theta : \mathbb{R}^d \rightarrow \mathbb{R}^k$ maps d input features to k output features, with weights θ . Given the input pair (x, y) drawn from the underlying distribution \mathcal{D} , f_θ predicts the label of x as $\hat{y} = \arg \max_{\{\hat{y}_1, \dots, \hat{y}_k\}} f_\theta(x)$. The correctness, robustness, violation, and robust accuracy of f_θ on (x, y) are defined as follows.

- **Correctness:** x is classified *correctly* if $\hat{y} = y$, where y is the true label.
- **Robustness:** f_θ is *robust* in the robustness region $B_\epsilon(x)$ around x if $\forall \tilde{x} \in B_\epsilon(x)$ f_θ always computes $\arg \max_{\hat{y}} f_\theta(\tilde{x}) = y$.
- **Violation:** If $\exists \tilde{x} \in B_\epsilon(x)$, such that $\arg \max_{\hat{y}} f_\theta(\tilde{x}) \neq y$, \tilde{x} is a *violation* of the robustness property.
- **Robust accuracy:** The expected percentage of test samples over the underlying distribution \mathcal{D} that is both correctly classified and have no violations within the corresponding robustness region B_ϵ .

The most common way to define a robustness region ($B_\epsilon(x)$) is to use a L_∞ -ball of radius ϵ around x [1]. However, the definitions presented above also apply to any arbitrary B_ϵ including other L_p norm-bounded balls.

The regular NN training process involves the objective function as shown in Eqn. 1, which optimizes the weights θ to minimize the expected risk of the loss value $\mathbb{E}_{(x,y) \sim \mathcal{D}}(L(\theta, x, y))$. The loss function $L(\theta, x, y)$ is used to measure the performance of the network on a specific input (x, y) . A correct prediction results in a very small loss value while incorrect predictions cause the loss values to be large. The cross-entropy loss function is commonly used to train the network. Since the underlying input distribution \mathcal{D} is unknown, the standard Empirical Risk Minimization (ERM) [23], [24] method uses the empirical distribution \mathcal{D}_0 , as represented by the training dataset of size N , to minimize the loss value $\mathbb{E}_{(x,y) \sim \mathcal{D}_0}(L(\theta, x, y)) = \frac{1}{N} \sum L(\theta, x, y)$.

$$\text{Regular Training Obj.} \quad \min_{\theta} \mathbb{E}_{(x,y) \sim \mathcal{D}}(L(\theta, x, y)) \quad (1)$$

$$\text{Robust Training Obj.} \quad \min_{\theta} \max_{\tilde{x} \in B_\epsilon(x)} \mathbb{E}_{(x,y) \sim \mathcal{D}}(L(\theta, \tilde{x}, y)) \quad (2)$$

By contrast, the robust training of NNs [25], [26], [20] minimizes the empirical risk of the largest loss value from B_ϵ (i.e., maximizes robust accuracy). Eqn. 1 and Eqn. 2 show the differences between the objective functions of regular and robust training. Specifically, The NN robust training tries to solve two related problems as shown by the objective function in Eqn. 2.

- **Inner Maximization Problem:** Finding \tilde{x} to maximize the loss value within a robustness region $B_\epsilon(x)$.
- **Outer Minimization Problem:** Optimizing weights θ to minimize the empirical maximal loss.

The inner maximization problem of the robust training procedure is known to be NP-hard [8]. Existing robust training approaches use either gradient-based attacks or sound over-approximations to find approximate solutions. The gradient-based attacks used by adversarially robust training schemes provide an under-approximation of the optimal solution, while verifiably robust training uses sound over-approximation techniques. Both of these training schemes use standard gradient descent and backpropagation for solving the outer minimization problem. We describe the details of each type of robustness, the corresponding threat models, and training procedures in detail in the rest of this section.

Note that just like the regular training process, robust training process also uses the empirical distribution \mathcal{D}_0 represented by the training dataset to compute the solutions to the inner/outer problems and expect that the solution will generalize to the underlying distribution. Also, both regular and robust training, instead of updating the NN weights for each training data sample separately, in practice, use batch training to make the training process more computationally efficient. The training data is split into batches of fixed size and for each batch of training data points $X = \{x_1, \dots, x_m\}$ and labels $Y = \{y_1, \dots, y_m\}$, the batch training procedure computes the loss value and performs back-propagation to update the weights to minimize the loss value.

B. Adversarial Robustness

Threat model. Besides bounding the perturbations by an attacker within the robustness region $B_\epsilon(x)$, adversarial robustness further assumes that the attacker is restricted to a specific subclass of attacks, i.e., first-order gradient-guided attackers. Recent works have trained NNs to be robust against different existing first-order attacks like Projected Gradient Descent (PGD) and Carlini-Wagner (CW) [27], [28], [29], [30]. Unfortunately, all of these defenses have been shown to be easily broken by slightly changing the corresponding attack exposing the inherent limitations of the underlying robust training schemes [31], [32].

To avoid such issues, Madry et al. [20] recently proposed a defense scheme against all first-order adversaries where the attacker is assumed to use first order gradients of the NN in arbitrary ways but not use any higher-order gradients. Madry et al. justified the choice of their threat model by arguing that computational complexity of higher-order gradients is not clearly understood and thus the memory and computation

cost may be significantly higher than computing first-order gradients. We summarize their robust training scheme below.

Adversarially robust training. The state-of-the-art adversarially robust training scheme of Madry et al. [20] relies on first-order gradient-guided PGD attacks to search for the largest loss value within B_ϵ . In fact, given input pair (x, y) , first-order attacks to estimate the lower bound of the inner maximization problem:

$$L(\text{Attack}(x), y) \leq \max_{\tilde{x} \in B_\epsilon(x)} L(f_\theta(\tilde{x}), y) \quad (3)$$

Specifically, for a batch of training data (X, Y) , the training process first conducts PGD perturbations with a random starting point to generate a perturbed training batch $X' = \text{PGD}(X)$, representing the estimated solution to the inner problem $\max_{\tilde{x} \in B_\epsilon(x)} L(f_\theta(\tilde{x}), y)$. The corresponding losses of X' and labels Y are then used to solve the outer minimization problem (Eqn. 2) using gradient descent by minimizing the function shown below.

$$\min_{\theta} \mathbb{E}_{(x,y) \sim \mathcal{D}} L(f_\theta(\text{PGD}(x)), y) \quad (4)$$

Madry et al.’s scheme is relatively efficient (though more expensive than regular training) and has been shown to be robust against known first-order attacks like Projected Gradient Descent (PGD) [27], Fast Gradient Sign Method (FGSM) [28], and Carlini-Wagner (CW) attacks [14]. In this paper, we define the *Estimated Robust Accuracy (ERA)* of a network as the percentage of test samples that are robust against known first-order attacks like PGD.

Limitations. Besides ignoring attacks using second- and higher-order derivatives, Madry et al.’s scheme also assumes that starting a first-order attack like PGD from a random starting point for each batch can provide a good solution to the inner maximization problem. To support this claim, they present experimental results from 100,000 random starting points showing that all solutions to the inner maximization problem found by PGD in these cases are distinct local optimas, yet they have very similar loss values. Due to the concentrated distribution of the loss values, Madry et al. concluded that the Projected Gradient Descent (PGD) attacker with a random start can be thought as the “ultimate” first-order adversary and thus can provide a good solutions to the inner maximization problem that can be achieved by arbitrary first-order attackers.

However, as NNs are non-convex, the solutions to the inner maximization problem found by a first-order attack like PGD can vary widely based on the starting point. Moreover, the non-convex nature of the NNs often make the *good* starting points to be very hard to find using random sampling used in Madry et al.’s experiment described earlier. In Section III-A), we present a new attack that uses first-order interval gradients to carefully good promising starting points for existing attacks like PGD. We show in Section III-A that the estimated *adversarial robust loss* value $L(f_\theta(\text{PGD}(x)), y)$ using PGD tend to be much smaller than the true maximal loss, as we will show in Section III-A. Moreover, we find that adapting the adversarially robust training process to use interval attacks converge

significantly slowly than the corresponding PGD version. This result exposes the fundamental limitation of such training methods. By contrast, our verifiably robust training scheme are more efficient and provides significantly stronger guarantees against stronger attackers than adversarially robust training.

C. Distributional Robustness

Threat model. Instead of defining the robustness region B_ϵ in terms of L-p norms, distributional robustness allows the adversary to draw any data samples (i.e., images) from a distribution P as long as it is within a bounded Wasserstein distance of ρ from the actual underlying data distribution \mathcal{D} [21]. Formally, the robustness region is $\mathcal{P} = \{P : W_c(P, \mathcal{D}) \leq \rho\}$. There is no other restriction on the information that the adversary has access to or the types of attack the adversary can perform.

Training scheme. Unfortunately, solving the inner maximization problem involving the Wasserstein distance is intractable. Therefore, To make the problem tractable, Sinha et al. [21] used the Lagrangian relaxation to reformulate the distribution distance bound into a L_2 distance penalty. Since \mathcal{D} is unknown, the authors used the empirical distribution \mathcal{D}_0 for computing the solutions.

Limitations. The distributional robust training provides an useful upper bound on the expectation of the loss function only when the bounded robustness region B_ϵ is very small (e.g., $\|\epsilon\|_2 \leq 0.1$). Such training become significantly ineffective as the bound becomes larger (e.g., $\|\epsilon\|_\infty \leq 0.1$). Moreover, the training methods require the NNs to have smooth activation functions like ELU and thus cannot support any networks using ReLUs, one of the most popular activation functions.

D. Verifiable Robustness

Threat model. Unlike the other two robustness definitions, verifiable robustness can provide protection against attackers with unlimited computation/information as long as the perturbations are limited within a robustness region $B_\epsilon(x)$. The attacker can use any information, draw input from arbitrary distributions, and launch unknown attacks.

Verifiably robust training. To capture the capabilities of unbounded attackers, sound analysis techniques are used to over-estimate the solutions to the inner maximization problem for a given the robustness region B_ϵ . The soundness ensures that no successful attack can be constructed within its B_ϵ input range if the analysis found no violations. Existing sound analysis techniques include convex polytope [18], symbolic intervals [7], [15], abstract domains [16], Lagrangian relaxation [33] and relaxation with Lipschitz constant [34]. Essentially, all of these perform a sound transformation T_ϵ from the input to the output of the network f_θ . Formally, given input $x \in \mathbb{X}$ and allowable input range $B_\epsilon(x)$, the transformation T_ϵ is sound if following condition is true:

$$\{f_\theta(\tilde{x}) | \tilde{x} \in B_\epsilon(x), \forall x \in \mathbb{X}\} \subseteq T_\epsilon(\mathbb{X}) \quad (5)$$

The verifiable robustness for an input pair (x, y) is defined as $\arg \max_{j \in \{1, \dots, k\}} d_\epsilon(x) = y$. It indicates that the output for class y for input x will always be predicted as the largest among all outputs estimated by sound over-approximation

$T_\epsilon(x)$. Here, $d_\epsilon(x)$ denotes the worst-case outputs produced by $T_\epsilon(x)$, which corresponds to the estimated worst regular loss value $L(d_\epsilon(x), y)$ within input range $B_\epsilon(x)$. Such sound over-approximations provide the upper bound of the inner maximization problem:

$$\max_{\tilde{x} \in B_\epsilon(x)} L(f_\theta(\tilde{x}), y) \leq L(d_\epsilon(x), y) \quad (6)$$

For a batch of training data points (X, Y) , the training process first computes the *verifiable robust loss* $L(d_\epsilon(X), Y)$ using sound over-approximation methods. Therefore, the outer minimization problem in Eqn. 2 becomes:

$$\min_{\theta} \mathbb{E}_{(x, y) \sim \mathcal{D}} L(d_\epsilon(x), y) \quad (7)$$

Such training increases the *Verified Robust Accuracy (VRA)* of a NN, the percentage of test samples within B_ϵ that can be verified using sound over-approximation to have no violations. The VRA provides a sound lower bound on the robust accuracy of a network as test samples might fail to verify due to false positives generated by over-approximation.

Limitations. While verifiably robust training schemes tend to achieve both high ERA and high VRA, existing training schemes are prohibitively expensive both in terms of computations and required memory, being hundreds of times slower than normal training methods. Moreover, due to the over-approximated violations, existing training schemes also sacrifice test accuracy to improve robustness. Such problems prevent these methods to be applied to real-world applications. In this paper, we specifically focus on verifiably robust training and propose two novel techniques that significantly cuts down the overhead of verifiably robust training while still achieving high accuracy and VRA.

III. INTERVAL ATTACK

In this section, we describe a novel interval-gradient-based attack against the state-of-the-art adversarially robust neural networks trained using Madry et al.’s [20] method. Their technique uses PGD attacks to find a maximal loss value for the inner maximization problem shown in Eqn. 2. As PGD is a first-order gradient-guided attack and the neural networks are non-convex, the maximal value found by the PGD might not be the optimal solution (i.e., the maximum) to the inner maximization problem. However, Madry et al. claimed that PGD attacks are the “ultimate” first-order attacks, i.e., no other first-order attack will be able to significantly improve over the solutions found by PGD. In order to support their claim, Madry et al. performed 100,000 iterations of the PGD attack from random starting points within bounded L_∞ -balls of test inputs and showed that all the solutions found by these instances are distinct local optimas with similar loss values. Therefore, they speculated that these distinct local optimas found by PGD attacks are very close to the best solution that can be found by any first-order attacker.

In this paper, we demonstrate that Madry et al.’s assumption that the solutions found by the PGD attacks cannot be improved by only using first-order information to be flawed.

Our first-order interval-gradient-based attack can effectively find *good* starting points for PGD attacks that significantly improves the attack success rate (up to 40% more) as opposed to starting from random points. Our experiments found that such starting points are not distributed evenly due to the non-convex nature of the neural networks and therefore are very hard to find using random sampling. Our attack demonstrates the pitfalls behind making assumptions about a neural network’s behavior, given its non-convexity, based on random sampling.

We further demonstrate that extending adversarial training method to use the interval attacks struggles to converge well (as shown in Figure 2) even after training for a extremely long time (12 hours) for a very small MNIST networks. We believe that this shows the fundamental limitations of adversarially robust training when used together with advanced attacks. By contrast, our verifiably robust training scheme does not make any such assumptions about the attacker and is more efficient than adversarially robust training schemes as shown in Section V.

Intuition behind interval attacks. Due to the non-convexity of the neural networks, existing first-order gradient-guided attacks like PGD and CW often get stuck at a local optima close to the starting point. Therefore, the loss value estimated by these attacks to solve the inner maximization problem might be significantly less than the true optimal value. Madry et al. try to mitigate such effects using a simple heuristic, i.e., picking a random starting point within the L_∞ ball for each instance of the attack. However, local optima and true optimal values of the inner maximization problem can be very unevenly distributed, the chances of reaching a better solution by simply randomly restarting the gradient-guided attacks is very low.

In this paper, we mitigate this problem, by using interval gradients instead of regular gradient to identify regions containing good starting points. Unlike regular gradients that summarize a function’s behavior at a point, interval gradients are computed over a region and thus have a broader view of the functional landscape. Compared to more computationally expensive information like second-order gradients, the interval gradient is still cheap to compute and relies only on first-order information. Figure 1a and Figure 1b illustrate how interval gradient can identify the regions containing potential violations that regular point-gradient-based search from a random starting point cannot find.

Our experiments confirm that the interval-gradient-guided search methods are more likely to find regions containing good starting points than random starts. However, interval-gradient-guided search cannot directly identify concrete attack inputs. We address this by first using interval gradients to find input regions containing good starting points and then launch existing attacks like PGD within that region to find concrete violations.

Interval gradient (g_I). Sound over-approximation techniques like symbolic interval analysis provides the lower and upper bounds (in terms of two parallel linear equations over symbolic inputs) of a neural network’s output for a bounded input region [7]. We define the interval gradient to be equal

to the slope of these parallel lines. In this paper, we use *symbolic linear relaxation*, which combines symbolic interval analysis with linear relaxation to provide tighter output bounds [15]. Essentially, such analysis produces two parallel linear equations (Eq_{up} and Eq_{low} as shown in Figure 1) to tightly bound the output of each neuron. For example, let us assume symbolic input relaxation provides the bounds of a neural network’s output as $[2x, 2x + 3]$ after propagating input range $x = [0, 1]$ through the network. Here, the interval gradient will be $\frac{d([2x, 2x+3])}{dx} = 2$.

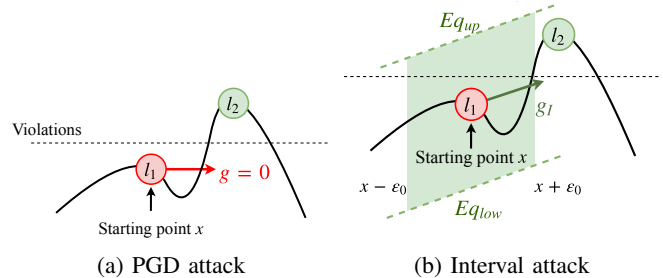


Fig. 1: **The difference between regular gradient and interval gradient. Figure (a) illustrates that PGD attacks using regular gradients might get stuck at l_1 . Figure (b) shows that interval gradient g_I over an input region B_{ϵ_0} allows us to avoid such problem and successfully locate the violation l_2 . Here Eq_{up} and Eq_{low} are the symbolic upper and lower bounds of the output as found by symbolic linear relaxation.**

Interval attack details. Algorithm 1 shows how we implemented the interval attack. The key challenge is to find a suitable value of ϵ_0 representing the input region over which the interval gradient will be computed (Line 3 to Line 7) at each iteration of interval-gradient-based search. If ϵ_0 is too large, the symbolic interval analysis will introduce large over-estimation error leading to the wrong direction. On the other hand, if ϵ_0 is too small, the information from the surrounding area might not be enough to make a clever update. Therefore, we dynamically adjust the size of ϵ_0 during the attack.

After a bounded number of iterations with interval gradients, we use PGD attack with a starting point from the region identified by the interval-gradient-based search to locate a concrete violation as shown in Line 13.

A. Effectiveness of Interval Attacks

We implemented symbolic interval analysis [15] and interval attacks on top of `Tensorflow 1.9.0`¹. All of our experiments are ran on a GeForce GTX 1080 Ti. We evaluated the interval attack on two neural networks MNIST_FC1 and MNIST_FC2. Both networks are trained to be adversarially robust using the Madry et al.’s technique [20]. For solving the inner maximization problem while robust training, we used PGD attacks with 40 iterations and 0.01 as step size. We define the robustness region, $B_\epsilon(x)$, to be bounded by L_∞ norm with $\epsilon = 0.3$ over normalized inputs. The network details are shown in Table I. We use the 1,024 randomly selected images from the MNIST test set to measure accuracy

¹<https://www.tensorflow.org/>

Algorithm 1 Interval Attack

Inputs: $x \leftarrow$ target input, $\epsilon \leftarrow$ attack budget
Parameters: t : iterations, α : step size, ϵ_0 : starting point, p : input region step size
Output: $x' \leftarrow$ perturbed x

```
1:  $x' = x$ 
2: for  $i \leftarrow 1$  to  $t$  do
3:    $\epsilon'_0 = \epsilon_0$ 
4:   // Find smallest  $\epsilon_0$  that might have violations
5:   while  $\text{argmax}(d_{\epsilon_0}(x)) = y$  do
6:      $\epsilon'_0 = \epsilon'_0 * p$ 
7:     if  $\epsilon'_0 >= \epsilon/2$  then break // Prevent  $\epsilon_0$  being too large
8:    $g_I = \nabla_x L(d_{\epsilon_0}(x'), y)$  // From symbolic interval analysis
9:    $x' = x' + \alpha g_I$ 
10:  // Bound  $x'$  within allowable input ranges
11:   $x' = \text{clip}(x', x - \epsilon, x + \epsilon)$ 
12:  if  $\text{argmax}(f_\theta(x')) \neq y$  then return  $x'$ 
13: PGD Attack( $x'$ )
14: return  $x'$ 
```

and robustness. MNIST_FC1 contains two hidden layers each with 512 hidden nodes. and achieves 98.0% test accuracy. Similarly, MNIST_FC2 contains five hidden layers each with 2,048 hidden nodes and achieve 98.8% test accuracy.

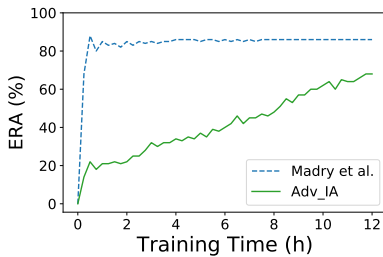


Fig. 2: Adversarially robust training using the interval attack does not converge well compared to using PGD attacks, given 12 hours of training time on the MNIST_Small network with $L_\infty \leq 0.3$. The estimated robust accuracy of training using PGD attacks [20] quickly converges to 89.3% ERA, while training using the interval attack struggles to converge.

Attack effectiveness. The interval attack is very effective at finding violations in both of our tested networks that are relatively robust against PGD and CW attacks with less than 35% success rate. We compared the strength of the interval attack against the state-of-the-art PGD and CW attacks given the same amount of attack time, as shown in Table I. The interval attack is able to achieve up to 40% increase in the attack success rate of PGD and CW. The iterations for PGD and CW are around 7,200 for MNIST_FC1 and 42,000 for MNIST_FC2. We ran the interval attack for 20 iterations against MNIST_FC1 and MNIST_FC2, which took 53.9 seconds and 466.5 seconds respectively.

Our results show that using only first-order gradient information, the interval attack can find significantly more robustness violations than PGD and CW attacks in adversarially robust networks.

Inefficiency of adversarially robust training with interval attacks. One obvious way of increasing the robustness

of adversarially robust trained networks against interval-based attacks is to use such attacks to solve the inner maximization problem during training. However, due to the highly uneven distribution of the loss values (as shown in Figure 3), robust training with interval attacks often struggle to converge. To demonstrate that, we evaluated adversarial robust training using interval attacks on MNIST_Small network for $L_\infty \leq 0.3$. As shown in the Figure 2, even after 12 hours training time for such a small network, the interval-based adversarially robust training does not converge as well as its PGD-based counterpart. Therefore, instead of improving the adversarially robust training schemes, we focus on scaling verifiably robust training, which can also defend against stronger attackers. In Section V-B, we show that MixTrain can achieve similar test accuracy with up to 95.2% more verified robust accuracy than existing adversarially robust training schemes, using $3\times$ less training time.

IV. METHODOLOGY

In this section, we discuss the design of MixTrain in detail. MixTrain is a generic defense that can work with any verifiably robust training methods to efficiently and scalably train robust neural networks. Specifically, we propose two key techniques, *Stochastic Robust Approximation* and *Dynamic Mixed Training*. Stochastic robust approximation significantly cuts down the overhead of sound over-approximations of violations with stochastic sampling. Similarly, dynamic mixed training helps the trained network to simultaneously achieve both high VRA and high test accuracy.

A. Motivation

Our design decisions for MixTrain are based on the observation that existing verifiably robust training methods suffer from two main scalability issues described below.

High computation and memory cost. Verifiably robust training uses sound over-approximation techniques like symbolic interval analysis, abstract interpretation, convex polytope etc. to solve the inner maximization problem as mentioned in Section II. All existing verifiably robust training schemes compute sound over-approximations of the network robustness for all training samples. This causes significant overhead both in terms of computation and memory. The state-of-the-art sound over-approximation techniques, despite impressive progress, are still hundreds of times slower and require thousands of times more memory than the regular forward propagation in a neural network [18], [19], [34], [15]. Most of the computational overhead in sound over-approximation techniques results from computing the precise bounds on the outputs of different hidden nodes of a network. Similarly, the amount of memory required for sound over-approximation increases significantly with the number of hidden nodes in a network. For instance, for verifiably robust training of a CIFAR residual network with around 32,000 hidden nodes requires up to around 300GB of memory while the regular training only needs 7MB.

Conflict between verifiable robustness and accuracy. We observe that verifiable robustness and test accuracy start conflicting after the initial training epochs, i.e., increasing

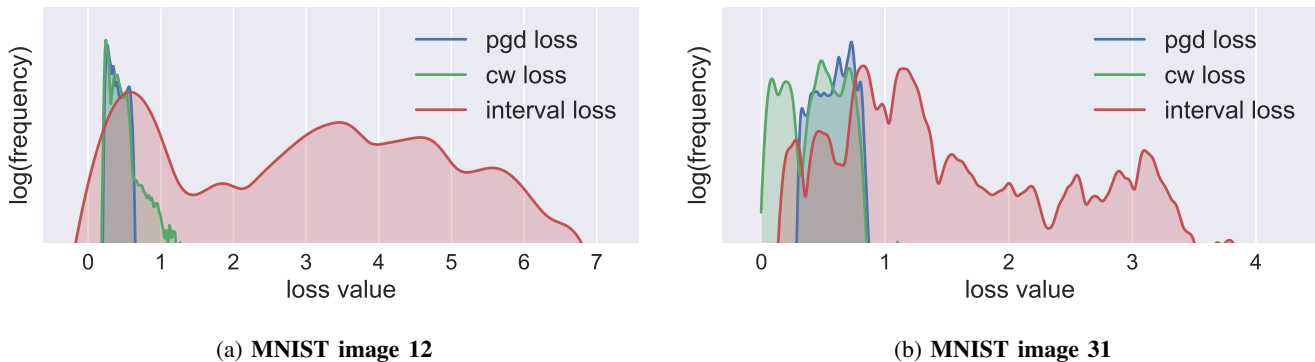


Fig. 3: Distributions of the loss values from robustness violations found by PGD attacks (blue), CW attacks (green), and interval attacks (red) with 100,000 random starts within the allowable input range $B_\epsilon(x)$. The loss values found by CW and PGD attacks are very small and concentrated. However, interval attacks show there are still many distinct violations with much larger loss values.

Network	# Hidden units	# Parameters	ACC (%)	Attack success rate (%)		
				PGD	CW	Interval attack
MNIST_FC1	1,024	668,672	98.1	39.2	42.2 (1.08 \times)	56.2 (1.43 \times)
MNIST_FC2	10,240	18,403,328	98.8	34.4	32.2 (0.94 \times)	44.4 (1.38 \times)

TABLE I: Attack success rates of PGD, CW and interval attacks ($\epsilon = 0.3$) on MNIST_FC1 and MNIST_FC2 networks. The highest success rates are in bold. Both networks are adversarially robust trained using PGD attacks with $\epsilon = 0.3$ [20].

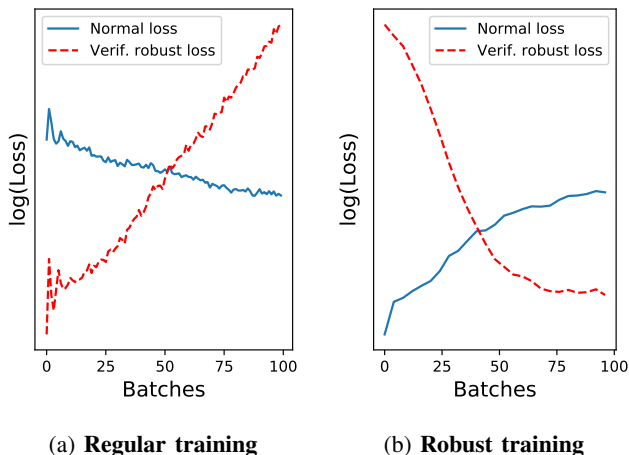


Fig. 4: The conflicting changes in regular loss and verifiable robust loss while training two CIFAR_Small networks. The left one is regular training after x epochs of verifiably robust training (Wong et al.’s method [19]) and the right one is verifiably robust training after x epochs of regular training.

one often decreases the other. Figure 4a and Figure 4b clearly shows this effect. For the first experiment, we start with a CIFAR_Small network pre-trained for 60 epochs with Wong et al.’s verifiably robust training method [19]. When we further trained this network with regular training, as shown in Figure 4a, the normal loss decreases (i.e., the test accuracy improves) but the verifiable robust loss increases (i.e., the VRA decreases). For the second experiment, we started with CIFAR_Small network pre-trained with regular training after 60 epochs. Training this network with verifiably robust training increases VRA but decreases test accuracy as shown by the loss values in Figure 4b. The results demonstrate that improving verifiable robustness and test accuracy becomes

conflicting after the initial training epochs.

B. Stochastic Robust Approximation

We propose *stochastic robust approximation* to reduce the computational and memory cost of the verifiable robust training process. The key insight behind our approach we should try to minimize the usage of expensive sound over-approximation methods without affecting the verified robustness of the final network. We observe that one does not actually need sound over-approximations of robustness violations over the entire training dataset during all intermediate steps of the training process. The verifiably robust training can efficiently minimize the verifiable robust loss as long as it is guided with sound over-approximation of robustness violations over a representative subset of the training data. Therefore, we use random subsampling to pick a representative subset of training data and use sound over-approximation process to estimate robustness violations over this subset. This step significantly speeds up the training process.

Stochastic robust approximation randomly samples k training data points as \mathcal{D}_k from \mathcal{D}_0 , i.e., n training data points. We find that the verifiable robust loss values computed over \mathcal{D}_k are representative of the verifiable robust loss values computed over the entire training dataset \mathcal{D}_0 .

Formally, let the \mathcal{D}_k denote the representative k data samples out of the entire training set \mathcal{D}_0 . Then, the new inner maximization problem for stochastic robust approximation can be defined as:

$$\max_{\tilde{x} \in B_\epsilon(x)} \mathbb{E}_{(x,y) \sim \mathcal{D}_k} L(d_\epsilon(x), y) \quad (8)$$

To test the effectiveness of subsampling to estimate robust loss over the entire training dataset, we randomly subsamples 1,000 data points ($k = 1,000$) out of 50,000 in CIFAR

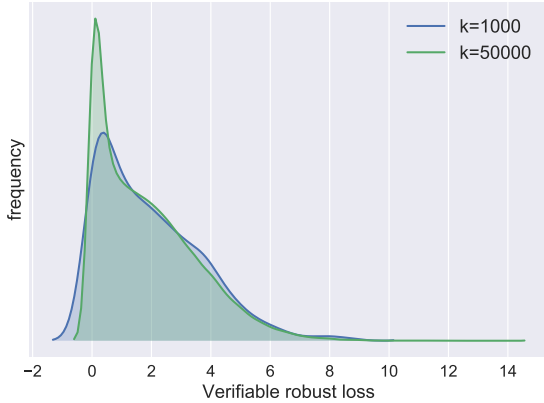


Fig. 5: The distributions of verifiable robust loss from the entire training set \mathcal{D}_0 and from the sampled training set \mathcal{D}_k ($k=1000$) are very similar.

training dataset. We compute the verifiable robust loss (i.e., estimated verifiable robustness violations) over both the subsampled data points and the entire training dataset. Figure 5 clearly shows that the distribution of verifiable robust loss \mathcal{D}_k over the sub-sampled set is very close to the loss distribution over the entire training dataset \mathcal{D}_0 . The two distributions significantly overlap and the verifiable robust loss values are between 0 to 2 for most of the data points.

Figure 5 clearly demonstrates that we can accurately estimate the verifiable robust loss values by computing sound over-approximation of the robustness violations over a randomly subsampled training dataset. This significantly reduces the time and memory requirements for MixTrain. For instance, by sampling $k = 1,000$ training data points out of 50,000, the computational cost of verifiably robust training gets down to 2% of the original cost using the entire training set.

Such finding is not surprising given that stochastic sampling is a common technique used in Machine Learning [35]. As we discussed in Section II, all training procedures for neural networks use sampling to perform the Empirical Risk Minimization (ERM) process for estimating the loss values over the underlying true distribution. Specifically, the n data points in the training dataset are assumed to be sampled from the underlying distribution \mathcal{D} and are treated as an empirical distribution \mathcal{D}_0 . Stochastic robust approximation simply takes such procedures one step further by subsampling the empirical distribution \mathcal{D}_0 for computing verifiable robust loss.

Integration with batch training. We further utilize the randomness in the batch generation process to integrate stochastic robust approximation with batch training that is commonly used for neural networks. Essentially, we pick k samples from different batches. Let m and n denote the batch size and the number of original training data points. Here, the training process will use $\frac{n}{m}$ batches. By distributing k random samples over these batches, we get $k' = \frac{k}{n/m}$ samples per batch. Before updating the weights of the neural network for each batch through back propagation, we compute the estimated

verifiable robust loss from k' random samples within the batch. For instance, in Figure 5, given batch size $m = 50$ and training dataset size $n = 50,000$, randomly sampling $k = 1,000$ from the training set is equivalent to randomly picking $k' = 1$ per batch. Our experimental results in Section V shows that setting $k' = 1$ achieves high VRA while running up to $14\times$ faster than the state-of-the-art verifiably robust training schemes [19]. stochastic robust approximation can be customized by changing the value of k as a hyperparameter.

C. Dynamic Mixed Training

Our second technique solves the conflict between the test accuracy and the verifiable robustness. Most state-of-the-art robust training schemes struggle to efficiently achieve both high test accuracy and high verifiable robustness [22], [17], [19]. To simultaneously increase both the test accuracy and the verifiable robustness, we dynamically balance the goals of training for each epoch using a dynamic loss function.

Specifically, we define our dynamic loss function as the following:

$$L_{mixed} = (1-\alpha) \mathbb{E}_{(x,y) \sim \mathcal{D}_0} L(f_{\theta}(x), y) + \alpha \mathbb{E}_{(x,y) \sim \mathcal{D}_k} L(d_{\epsilon}(x), y) \quad (9)$$

L_{mixed} is a weighted sum of the expectation of both the regular loss $\mathbb{E}_{(x,y) \sim \mathcal{D}_0} L(f_{\theta}(x), y)$ and the verifiable robust loss $\mathbb{E}_{(x,y) \sim \mathcal{D}_k} L(d_{\epsilon}(x), y)$. The hyperparameter α , which takes a value between 0 and 1, biases the dynamic loss value towards either regular loss or verifiably robust loss. When α is large, the training process tends to find the weights θ that minimize the verifiable robust loss, increasing VRA. In contrast, if α is small, Eqn. 9 emphasizes more on the regular loss and thus enhances the test accuracy.

Dynamic Loss. We dynamically adjust α per epoch to prioritize different emphasis on the regular loss and the verifiably robust loss. The dynamic loss function allows us to adaptively maximize the test accuracy and VRA simultaneously based on the the current test accuracy. It can balance the gradients generated from the loss of both the regular and the verifiably robust training tasks. Therefore, we can avoid the training being completely dominated by the one with a larger gradient. Using dynamic loss, we are able to robustly train the networks that have up to 13.2% higher test accuracy compared to the state-of-the-art verifiably robust training schemes [19] with similar VRA (Section V). Besides the test accuracy improvement, another significant benefit of MixTrain is that it helps convergence of the training process especially when either the regular loss or verifiably robust loss functions are difficult to optimize by themselves.

In our experiments, we use a specific α function as defined in Section V-B. In general, α can be any reasonably smooth function. For example, grid search can be used to find the best α for each epoch. Alternatively, the best α for different epochs and different networks can potentially be policies learned using reinforcement learning techniques. We leave exploring these directions as future work.

V. EVALUATION

We implemented stochastic robust approximation and dynamic mixed training as part of MixTrain, built on PyTorch 0.4.0². In MixTrain, we used symbolic linear relaxation as the sound over-approximation method proposed by Wang et al. [15]. In this section, we evaluate MixTrain on 6 different networks trained over 3 different datasets and compare MixTrain’s performance against 4 state-of-the-art verifiably and adversarially robust training methods. We compare these robust training techniques against MixTrain using three metrics: test accuracy (ACC), estimated robust accuracy under PGD attacks (ERA), and verified robust accuracy (VRA). Unless otherwise specified, we use ERA to denote the robust accuracy as measured with PGD attacks for the rest of the paper. We summarize our main results below:

- 1) Compared to the state-of-the-art adversarially robust training methods [20], [21] that have zero VRA, MixTrain can obtain up to 95.2% VRA with similar ERA(PGD) and ACC, using 3 times less training time on average.
- 2) Compared to state-of-the-art verifiably robust training methods [19], [17], MixTrain can achieve up to 13.2% higher ACC and 6.5% higher VRA, allowing verifiably robust networks to be trained for real-world applications.
- 3) MixTrain requires, on average, 10 times less training time compared to state-of-the-art verifiably robust training schemes [19] and thus can easily scale to large network trained on the ImageNet-200 dataset. For such large network, MixTrain outperforms the existing verifiably robust training methods by up to 14.3% VRA within 12-hour of training time.

A. Experimental Setup

Network	Type	# hidden units	# parameters
MNIST_Small	Conv	4,804	166,406
MNIST_large	Conv	28,064	1,974,762
CIFAR_Small	Conv	6,244	214,918
CIFAR_Large	Conv	62,464	2,466,858
CIFAR_Resnet	Residual	31,720	1,145,410
ImageNet_Resnet	Residual	172,544	2,310,664

TABLE II: Architectures of the 6 neural networks used for evaluating MixTrain.

Datasets & networks. We evaluate MixTrain on three different datasets: MNIST digit classification [36], CIFAR10 image classification [37] and ImageNet-200³ [38]. We use six different network architectures for the experiments. The details of the networks are shown in Table II. We refer the interested readers to Appendix B for further details.

Unless otherwise specified, similar to Wong et al. [19], we train 60 epochs in total with batch size of 50 for all experiments. We follow the standard normalization procedures

(described below before training for all of the datasets [19], [22], [20], [21]). For the MNIST dataset, we scale the inputs to be within $[0, 1]$ with $\mu = 0.5$. We use the Adam optimizer [39] with learning rate 0.001 and decay it by a factor of 0.6 for every 5 epochs. We use ϵ starting from 0.01 to the values used for measuring VRA over the first 10 epochs⁴. Similarly, for the CIFAR dataset, we normalize inputs with $\mu = [0.485, 0.456, 0.406]$, $\sigma = [0.225, 0.225, 0.225]$. We use the SGD optimizer [40], [41] with learning rate 0.05 and decay it by 0.6 for every 5 epochs. We use ϵ starting from 0.001 to values used for measuring VRA over the first 10 epochs. We use the same configurations for ImageNet-200 dataset too. All of our experiments are ran on a GeForce GTX 1080 Ti. For all networks trained using the same dataset, we use the configurations as well as the same randomly selected set of test images to compute ACC, ERA, and VRA.

Dynamic α function of MixTrain. We used the following α function for MixTrain’s dynamic loss function:

$$\alpha_t = \begin{cases} \alpha_0, & \text{if } t = 0 \\ \alpha_{t-1} + 0.05, & \text{if } acc > acc_0 \\ \alpha_{t-1} - 0.05, & \text{if } acc \leq acc_0 \end{cases}$$

Here acc denotes the accuracy of a sub-sampled training dataset for the current epoch t . acc_0 and α_0 denote the desired accuracy and the initial α value, respectively. In this conditional function, α takes an initial value of α_0 at the beginning (i.e., $t = 0$) of the batch training process. Afterwards, for each epoch, α changes according to the accuracy of current epoch. When the test accuracy increases and becomes larger than targeted acc_0 , we increase α by 0.05. Similarly, if the test accuracy decreases and becomes less than acc_0 , we deduct 0.05 from the current value of α .

Since the MNIST networks, unlike the other networks we tested, can be easily trained to have high test accuracy, we want MixTrain to spend more effort on improving verifiable robustness in dynamic mixed training. Therefore, we set α_0 to be 0.8. By contrast, for CIFAR networks, where achieving high accuracy is hard, we set α_0 to 0.5.

B. MixTrain vs. state-of-the-art training schemes

For each network architecture in Table II, we compared the performance of MixTrain with existing state-of-the-art schemes: two adversarially robust training schemes by Madry et al. [20] and Sinha et al. [21] and two verifiably robust training schemes by Wong et al. [19] and Mirman et al. (DIFFAI) [17].

For the two adversarially robust training schemes, we used the same adversary configurations and training process from Madry et al. [20]. For the two verifiably robust training schemes, we picked the experimental setup that achieved the best results as described in the corresponding paper. Wong et al.’s method [19] is the state-of-the-art at supporting verifiable robustness, i.e., VRA. We used 50 random projections for

²<https://pytorch.org/>

³Imagenet-200 is a subset of the ImageNet dataset with 200 classes instead of 1,000. Also, each piece of training data is cropped to be $3 \times 64 \times 64$.

⁴Since sound over-approximations over a network during the early stages of training is more expensive than later stages, decaying ϵ is necessary to bootstrap the training process.

Network	Epsilon	Method	Batch Time (s)	Training Time	ACC (%)	ERA (%)	VRA (%)
MNIST_Small	0.1	Regular training	0.006	7m12s	98.6	0.8	0
		Madry et al. [20]	0.027	32m4s	99.1	96.0	0
		Sinha et al. [21]	0.026	31m12s	98.7	58.5	0
	MixTrain	0.011	13m12s	98.5	96.3	91.6	
	0.3	Madry et al. [20]	0.027	32m24s	98.8	89.3	0
		Sinha et al. [21]	0.026	31m12s	98.9	0	0
MixTrain		0.011	13m48s	95.4	87.3	52	
MNIST_Large	0.1	Regular training	0.007	8m24s	99.3	26.8	0
		Madry et al. [20]	0.063	1h15m	98.9	96.7	0
		Sinha et al. [21]	0.063	1h16m	99.0	70.1	0
		MixTrain	0.051	1h1m	99.5	98.2	95.2
	0.3	Madry et al. [20]	0.063	1h15m	Does not converge		
		Sinha et al. [21]	0.066	1h19m	99.1	0.1	0
CIFAR_Small	0.0348	MixTrain	0.054	1h5m	96.6	89.4	58.4
		Regular training	0.011	10m57s	77.3	18.6	0
		Madry et al. [20]	0.194	3h15m	71.2	54.3	0
		Sinha et al. [21]	0.192	3h11m	71.8	11.3	0
CIFAR_Large	0.0348	MixTrain	0.015	14m52s	71.1	54.6	37.6
		Regular training	0.012	12m3s	86.4	14.3	0
		Madry et al. [20]	0.289	4h49m	80.9	63.6	0
		Sinha et al. [21]	0.204	3h24m	75.1	13.7	0
CIFAR_Resnet	0.0348	MixTrain	0.239	3h59m	77.9	63.5	41.6
		Regular training	0.014	14m39s	84.2	22.6	0
		Madry et al. [20]	0.306	5h6m	Does not converge		
		Sinha et al. [21]	0.212	3h32m	77.3	17.7	0
MixTrain	0.109	1h49m	77.5	61.0	35.5		

TABLE III: Comparison between MixTrain and existing state-of-the-art adversarially robust training methods. The best robust training numbers are shown in bold. Compared to the adversarially robust trained networks, after training 60 epochs, MixTrain with $k=1$ can provide similar test accuracy and ERA with up to 95.2% more verifiable robustness within shorter training time.

Wong et al.’s method [19]. Similarly, we use training with box domains and testing with a hybrid Zonotope domain with transformer method hSwitch for DIFFAI [17] since this achieved the best results.

Comparison with Adversarially Robust Training. In Table III, we have shown the training results of different techniques for the five tested networks. The best training time and VRA are highlighted for each network. Here, k of stochastic robust approximation is set to be 1 to maximize the training process’s efficiency.

When training the MNIST_Large network with $\epsilon = 0.3$ and CIFAR_Resnet, Madry et al.’s method [20] does not converge. We cannot find a feasible choice of learning rate ($lr = 10^{-7}, 3 \times 10^{-7}, 10^{-6}, \dots, 10$) that can train the network to have over 30% test accuracy.

As shown by the results in Table III, MixTrain obtain the highest VRA for all networks. Madry et al.’s method [20] is efficient but it cannot provide any verifiable robustness, i.e., has zero VRA. By contrast, MixTrain can get VRA as high as 95.2% while still being faster than Madry’s method achieving same ACC and ERA. Such improvement in verifiable robustness is highly significant especially for security-sensitive applications. The training schemes of Sinha et al. [21] can reach higher ERA scores when $\epsilon = 0.1$ compared to $\epsilon = 0.3$ for MNIST networks. However, on CIFAR networks, it performed much worse in terms of ERA than MixTrain and Madry et al.’s method [20]. This is consistent with the results reported in [21] as the distributional robustness works well for only very small ϵ values. Note that MixTrain is faster

than the other two adversarially robust training schemes on all networks except CIFAR_Large. Sinha et al.’s method [21] is slightly faster than MixTrain on CIFAR_Large, but we have significantly higher ACC, ERA, and VRA scores.

Comparison with Verifiably Robust Training. In Table IV, we compared the performance of MixTrain against verifiably robust training methods within 12-hours training time. Despite high VRA, currently the best verifiably robust trained networks provided by Wong et al. [19] still suffer from scalability issues and low test accuracy. Table IV clearly demonstrates that stochastic robust approximation and dynamic mixed training are two very powerful methods that allow us to scale to large networks and balance the VRA and test accuracy. Note that the results for DIFFAI on MNIST dataset are lower than the numbers reported in [17] mainly because their input normalization have a different scale (e.g., their $\epsilon = 0.3$ only maps to L_∞ norm of 25 out of 255 before normalization while our $\epsilon = 0.3$ maps to $L_\infty = 76$). Though DIFFAI with box domains are efficient to train, our experiments show that they tend to introduce large overestimation errors. Therefore, VRA of DIFFAI is low for most of the networks. Moreover, DIFFAI does not converge on MNIST_Large and CIFAR_Large networks.

While running stochastic robust approximation on small networks (MNIST_Small, CIFAR_Small), we set k to be 20 to compute the verifiable robust loss without increasing the training cost too much. For the larger networks like CIFAR_Resnet and CIFAR_Large, we pick $k = 10$. Note that we can make k larger to further improve the VRA by spending more training time. For MNIST_Large, we find that

Network	ϵ	Method	Batch Time (s)	Training Time	ACC (%)	ERA (%)	VRA (%)
MNIST_Small	0.1	DIFFAI [17]	0.013	12h	97.8	93.1	60.6
		Wong et al. [19]	0.078	12h	98.6	96.9	95.7
		MixTrain	0.026	12h	99.5	98.0	97.1
	0.3	DIFFAI [17]	0.012	12h	98.2	82.9	0
		Wong et al. [19]	0.079	12h	91.2	83.1	57.8
		MixTrain	0.028	12h	94.0	86.1	60.1
MNIST_Large	0.1	DIFFAI [17]	0.022	12h	Does not converge		
		Wong et al. [19]	0.687	12h	99.2	98.3	96.4
		MixTrain	0.051	12h	99.5	98.2	95.2
	0.3	DIFFAI [17]	0.023	12h	Does not converge		
		Wong et al. [19]	0.689	12h	86.6	71.7	53.1
		MixTrain	0.054	12h	96.6	89.4	58.4
CIFAR_Small	0.0348	DIFFAI [17]	0.015	12h	66.3	41.9	4.0
		Wong et al. [19]	0.248	12h	62.5	52.3	47.5
		MixTrain	0.087	12h	69.4	56.5	48.2
CIFAR_Large	0.0348	DIFFAI [17]	0.025	12h	Does not converge		
		Wong et al. [19]	2.157	12h	61.9	56.4	49.4
		MixTrain	0.268	12h	74.1	62.7	50.2
CIFAR_Resnet	0.0348	DIFFAI [17]	0.035	12h	75.6	35.8	0.0
		Wong et al. [19]	1.914	12h	58.1	51.7	43.9
		MixTrain	0.281	12h	71.3	60.5	50.4

TABLE IV: Comparison between state-of-the-art verifiably robust training methods and MixTrain. The best numbers are shown in bold. With 12 hours of training time, compared to the verifiably robust trained networks, MixTrain can achieve up to 13.2% ACC improvements and 6.5% VRA improvements.

Network	ϵ	Method	Training Time	Others	ACC (%)
				MixTrain	
MNIST_Small	0.1	DIFFAI [17]	>24h	>36×	N/A
		Wong et al. [19]	>24h	>36×	N/A
		MixTrain	39m26s	-	99.5
	0.3	DIFFAI [17]	>24h	>28×	N/A
		Wong et al. [19]	>24h	>28×	N/A
		MixTrain	50m12s	-	94.0
MNIST_Large	0.1	DIFFAI [17]	>24h	>26×	N/A
		Wong et al. [19]	3h59m	4×	98.9
		MixTrain	55m12s	-	99.5
	0.3	DIFFAI [17]	>24h	>24×	N/A
		Wong et al. [19]	>24h	>24×	N/A
		MixTrain	58m35s	-	96.6
CIFAR_Small	0.0348	DIFFAI [17]	>24h	>16×	N/A
		Wong et al. [19]	3h35m	3×	61.3
		MixTrain	1h25m	-	69.4
CIFAR_Large	0.0348	DIFFAI [17]	>24h	>5×	N/A
		Wong et al. [19]	13h14m	3×	64.9
		MixTrain (k=10)	4h28m	-	74.1
CIFAR_Resnet	0.0348	DIFFAI [17]	>24h	>5×	N/A
		Wong et al. [19]	15h53m	3×	60.2
		MixTrain	4h36m	-	71.3

TABLE V: The shortest training time needed by different verifiable robust training schemes to achieve the same VRA as what MixTrain achieved in Table IV, along with the corresponding test accuracy.

$k = 1$ is enough to outperform the existing state-of-the-art.

For all networks, within 12-hour training time, MixTrain achieved higher ACC and VRA than DIFFAI and Wong et al.’s method. In particular, we have achieved 4.2% higher VRA and 9.2% higher ACC than the best reported number of Wong et al. [19] for the MNIST_Large network ($\epsilon = 0.3$). **Time to Achieve Target VRA.** We test whether other verifiably robust training methods can reach the same VRA

as MixTrain if we allow more training time. We set the training time threshold to be 24 hours and set the target VRA for all verifiably robust training methods to be those achieved by MixTrain in Table IV. The results are shown in Table V. MixTrain, on average, is 15× faster than Wong et al.’s method [19] and at least 20× faster than DIFFAI for reaching the same target VRA.

Results for ImageNet-200. All existing verifiably robust training methods have so far been only evaluated on the MNIST and CIFAR dataset. Since the training cost of verifiably robust networks increase drastically for large datasets like ImageNet [42], [43]) and thus training networks with significant verifiable robustness is very hard. We evaluate MixTrain with ImageNet_Resnet trained on the Imagenet-200 [38] dataset and show that MixTrain can scale to such large networks. We use robustness regions bounded by $L_\infty \leq 0.007^5$. We set $k=5$ and train the networks for 12 hours. As shown in Table VI, MixTrain outperforms the state-of-the-art verifiable robust training methods by up to 11.8% test accuracy and 14.4% verified robust accuracy.

Method	Batch Time (s)	ACC (%)	VRA (%)
Regular training	0.022	36.2	0
Wong et al. [19]	3.392	14.4	5.1
MixTrain	0.396	26.2	19.4

TABLE VI: The test accuracy (ACC) and verified robust accuracy (VRA) of ImageNet_Resnet network trained with 12 hours using the ImageNet-200 dataset with $\epsilon \leq 0.007$.

⁵the same robustness region is used in [17] for the CIFAR dataset.

C. Robustness for different L_∞ bounds

We examine the VRA and ERA metrics with different robustness regions in the CIFAR_Large and MNIST_Large networks trained with MixTrain. The CIFAR_Large network and MNIST_Large are trained with $L_\infty \leq 0.0348$ and $L_\infty \leq 0.3$, respectively. Figure 6 shows that these two networks have high VRA and ERA scores within large L_∞ bounds. Overall, the ERA values are higher than VRA. For MNIST_Large, the VRA score is still over 80% when ϵ is 0.25. Similarly for CIFAR_Large, the VRA score is higher than 60% when ϵ is 0.025. Note that the verifiable robustness of MNIST_Large decreases faster than CIFAR_Large’s, since the training range $L_\infty \leq 0.3$ is relative large that covers almost all visually undetectable perturbations.

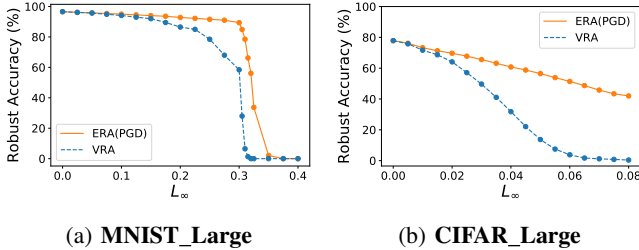


Fig. 6: Changes of ERA and VRA in different ϵ regions of MNIST_Large and CIFAR_Large networks trained with MixTrain.

D. MixTrain vs. state-of-the-art attacks

We show in Table VII that MixTrain can effectively defend against the state-of-the-art attacks including PGD, CW and interval attacks. For the same configurations of attacks, the interval attacks can find up to $1.4\times$ as many violations as PGD/CW attacks on adversarially robust trained networks as shown in Table I. However, such advantage in success rate decreases to be less than 1% on the networks trained with MixTrain. It indicates that, compared to Madry et al.’s method [20], MixTrain increases the verifiable robustness of networks to make them more robust and reliable under unknown attacks.

Network	ACC (%)	ERA (PGD) (%)	ERA (CW) (%)	ERA (IA)* (%)	VRA (%)
MNIST_Small	95.4	87.3	87.2	86.7	52.0
MNIST_Large	96.6	89.4	90.0	88.6	58.4
CIFAR_Small	71.1	54.6	53.9	53.1	37.6
CIFAR_Large	77.9	63.5	62.8	62.2	41.6
CIFAR_Resnet	77.5	61.0	60.4	59.6	35.2

* Estimated robust accuracy under interval attacks.

TABLE VII: ERA of networks trained with MixTrain under different attacks (ϵ is 0.3 for MNIST and 0.0348 for CIFAR).

E. MixTrain against L_0 and L_2 bounded attacks

Using L_∞ -bound for verifiably robust training, MixTrain can also make networks robust against L_0 and L_2 -bounded attacks. Schott et al. [32] have shown that Madry et al.’s method [20] is not robust against other types of attacks like L_0 and L_2 -bounded attacks. In Figure 7, we measure the ERA under state-of-the-art L_2 -bounded CW attacks and

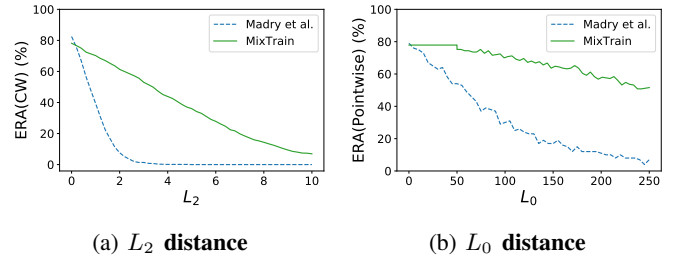


Fig. 7: ERA of CIFAR_Large networks trained with MixTrain vs Madry et al. [20], under L_2 -bounded CW attacks and L_0 -bounded pointwise attacks. As additional benefits, the networks trained with MixTrain are much more robust against L_0 and L_2 adversaries.

L_0 -bounded decision-based pointwise attacks [32], [44] on CIFAR_Large networks trained with MixTrain. We compare the differences of the ERA obtained through MixTrain against the networks trained from Madry et al.’s method [20]. For L_2 -bounded CW attacks, as shown in Figure 7a, the ERA of adversarially robust trained network quickly decreases to 0% when $L_2 = 2$, whereas MixTrain can retain over 60% ERA. For L_0 -bounded pointwise attacks, as shown in Figure 7b, ERA of the network trained with MixTrain stays over 50% at $\epsilon = 250$ while Madry et al.’s number drops to 0%. The results demonstrate that the networks trained with MixTrain are much more robust against L_0 and L_2 adversaries as side benefits of MixTrain under L_∞ -bounded sound over-approximations.

F. Different values of sampling rate k

We evaluate different choices of k in stochastic robust approximation over the resulting accuracy metrics and training time in Table VIII. Larger k values can increase ERA and VRA scores at the cost of more training time. In particular, we train the CIFAR_Small networks with MixTrain on one GPU. When $k = 1$, the network achieves 71.1% test accuracy and decent VRA (37.6%), with very efficient training time. Therefore, $k = 1$ is a good choice to save training time/memory. On the other hand, if more training time is available, one can use larger sampling rate k to obtain higher VRA. For instance, with $k = 20$, MixTrain can train a robust network with a high VRA (45.4% vs 47.5%) and a significantly higher test accuracy (70.7% vs 61.1%) compared to the state-of-the-art method by Wong et al. [19]. Also, it only takes MixTrain 2 hours and 42 minutes to train whereas existing verifiable robust training techniques need over 11 hours to reach the same VRA.

	Batch Time (s)	Training Time	ACC (%)	ERA (%)	VRA (%)
k=1	0.015	14m52s	71.1	54.6	37.6
k=5	0.042	45m23s	70.7	54.9	39.9
k=10	0.078	1h18m	69.7	55.2	43.2
k=20	0.162	2h42m	70.7	56.7	45.4

TABLE VIII: Under different values of sampling rate k for stochastic robust approximation, the comparisons of corresponding training time, ACC, ERA, and VRA on CIFAR_Small networks.

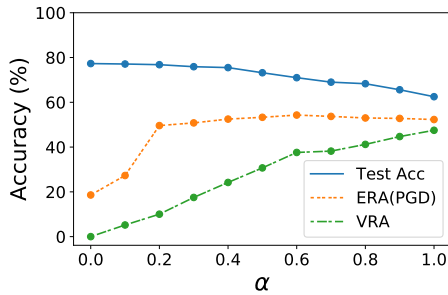


Fig. 8: ACC, ERA, and VRA of CIFAR_Small networks trained with MixTrain under different fixed α values in dynamic mixed training.

G. Different values of α

Influence of different α values. We measure how ACC, ERA, and VRA change with different fixed α values used for training the CIFAR_Small network. Specifically, we use different constant values $\alpha = 0.0, 0.1, \dots, 1.0$ to evaluate the corresponding metrics of each network trained with $k = 1$. Figure 8 shows that as α increases, both ERA and VRA increase but test accuracy decreases. If $\alpha = 0$, the training process is the same as regular training, which has the highest ACC but 0% VRA. By contrast, if $\alpha = 1$, MixTrain only relies on stochastic robust approximation and loses the ACC improvement provided by dynamic mixed training. Overall, by adjusting α , MixTrain can be tuned to balance the verifiable robustness and test accuracy as desired.

Dynamic update of α . Instead of using a fixed α value in training, dynamically changing α can achieve higher ERA and VRA. In Table IX, we compare the results achieved by dynamic α with those by a fixed α . First, we train with a fixed $\alpha = 0.5$ that balances between ACC and VRA of the network. Next, we adaptively update α as described in Section V-A and compare the resulting ACC, ERA, and VRA metrics. As shown in Table IX, the network trained with dynamic α outperforms the network trained under fixed α mechanisms by 6.7% VRA while achieving similar ACC.

CIFAR_Small	ACC (%)	ERA (%)	VRA (%)
Fixed $\alpha = 0.5$	71.4	53.2	30.9
Adaptive α	71.7	54.6	37.6

TABLE IX: Performance of CIFAR_Small networks trained with dynamically adapted α vs fixed α .

VI. RELATED WORK

Recent works have shown that the state-of-the-art neural networks can be easily fooled with adversarially crafted human-imperceptible perturbations on valid inputs [14], [1], [28], [13]. The proposed defenses can be categorized into two classes—best-effort defenses and principled defenses satisfying some security properties.

Best-effort defenses. Defenses of this class usually rely on heuristics without supporting any clear security guarantees about the robustness of the underlying network to adversarial inputs [45], [9], [10], [46], [47], [31], [48], [49], [50], [51].

Therefore, these defenses have been followed by a sequence of stronger attacks breaking them in quick succession [52], [14], [53], [54], [13], [55], [56], [12], [57], [58], [59], [60], [61], [62]. We refer the interested readers to the survey by Athalye et al. [31] for more details.

Principled defenses. Adversarially robust training and verifiably robust training are the two main classes of principled defenses. Adversarially robust training uses various different existing attacks [28], [27], [29], [30], [56], [20] to make the trained network robust. Overall, they are robust against existing attacks [20], but can still be defeated by smarter attackers as shown in this paper.

Verifiably robust training can provide sound estimates of the robustness of the trained network. They use sound over-approximation of violations to guide the training process. The underlying techniques for soundly measuring robustness include basic linear programming [63], SMT solvers [8], [64], [65], MILP solvers [66], [67], [68], semidefinite relaxations [69], symbolic intervals [7], [15], convex polytopes [18], abstract domains [16], Lagrangian relaxations [33] and Lipschitz continuity [70], [34]. To increase the efficiency of the training process, verifiably robust training often has to make some sacrifice in the soundness of the robustness estimates [22], [17]. Currently, the state of the art, leveraging random projections to save computations [19], is still hundreds of times slower than regular training. MixTrain speeds up the verifiably robust training by on average 15 times with up to 13.2% test accuracy improvement.

VII. CONCLUSION

In this paper, we designed, implemented, and evaluated stochastic robust approximation and dynamic mixed training as part of MixTrain for making verifiably robust training of neural networks an order of magnitude faster. Our extensive experimental results demonstrated that MixTrain outperforms the state-of-the-art verifiably robust training methods achieving 13.2% improvement in test accuracy and up to 6.5% higher verified robust accuracy while taking $36\times$ less training time and $50\times$ less memory. MixTrain even takes up to $2x$ less training time than the state-of-the-art adversarially robust training methods that cannot provide any verified robustness accuracy. We further presented a new first-order attack, the interval attack, that shows the fundamental limitations of adversarially robust training [20]. By contrast, MixTrain provides strong security any L-p-norm bounded attacks including interval attacks.

REFERENCES

- [1] C. Szegedy, W. Zaremba, I. Sutskever, J. Bruna, D. Erhan, I. Goodfellow, and R. Fergus, “Intriguing properties of neural networks,” *International Conference on Learning Representations (ICLR)*, 2013.
- [2] “TESLA’S AUTOPILOT WAS INVOLVED IN ANOTHER DEADLY CAR CRASH,” <https://www.wired.com/story/tesla-autopilot-self-driving-crash-california/>.
- [3] “Driver killed in Tesla self-driving car crash ignored warnings, NTSB reports,” <https://www.usatoday.com/videos/news/nation/2017/06/20/tesla-found-not-fault-fatal-self-driving-car-crash/103039630/>.
- [4] “Uber’s Self-driving Car Were Struggled Before Arizona Crash,” <https://www.nytimes.com/2018/03/23/technology/uber-self-driving-cars-arizona.html>.

- [5] K. D. Julian, J. Lopez, J. S. Brush, M. P. Owen, and M. J. Kochenderfer, "Policy compression for aircraft collision avoidance systems," in *Digital Avionics Systems Conference (DASC), 2016 IEEE/AIAA 35th*. IEEE, 2016, pp. 1–10.
- [6] "NAVAIR plans to install ACAS Xu on MQ-4C fleet," <https://www.flightglobal.com/news/articles/navair-plans-to-install-acas-xu-on-mq-4c-fleet-444989/>.
- [7] S. Wang, K. Pei, W. Justin, J. Yang, and S. Jana, "Formal security analysis of neural networks using symbolic intervals," *27th USENIX Security Symposium*, 2018.
- [8] G. Katz, C. Barrett, D. L. Dill, K. Julian, and M. J. Kochenderfer, "Reluplex: An efficient smt solver for verifying deep neural networks," in *International Conference on Computer Aided Verification (CAV)*. Springer, 2017, pp. 97–117.
- [9] N. Papernot, P. McDaniel, X. Wu, S. Jha, and A. Swami, "Distillation as a defense to adversarial perturbations against deep neural networks," *arXiv preprint arXiv:1511.04508*, 2015.
- [10] M. Cisse, P. Bojanowski, E. Grave, Y. Dauphin, and N. Usunier, "Parseval networks: Improving robustness to adversarial examples," in *International Conference on Machine Learning (ICML)*, 2017, pp. 854–863.
- [11] M. Lecuyer, V. Atlidakis, R. Geambasu, H. Daniel, and S. Jana, "Certified robustness to adversarial examples with differential privacy," *arXiv preprint arXiv:1802.03471*, 2018.
- [12] N. Papernot, P. McDaniel, I. Goodfellow, S. Jha, Z. B. Celik, and A. Swami, "Practical black-box attacks against machine learning," in *Proceedings of the 2017 ACM on Asia Conference on Computer and Communications Security*. ACM, 2017, pp. 506–519.
- [13] S.-M. Moosavi-Dezfooli, A. Fawzi, and P. Frossard, "Deepfool: a simple and accurate method to fool deep neural networks," in *Proceedings of the IEEE Conference on Computer Vision and Pattern Recognition (CVPR)*, 2016, pp. 2574–2582.
- [14] N. Carlini and D. Wagner, "Towards evaluating the robustness of neural networks," in *IEEE Symposium on Security and Privacy (SP)*. IEEE, 2017, pp. 39–57.
- [15] S. Wang, K. Pei, W. Justin, J. Yang, and S. Jana, "Efficient formal safety analysis of neural networks," *Advances in Neural Information Processing Systems (NIPS)*, 2018.
- [16] T. Gehr, M. Mirman, D. Drachler-Cohen, P. Tsankov, S. Chaudhuri, and M. Vechev, "Ai 2: Safety and robustness certification of neural networks with abstract interpretation," in *IEEE Symposium on Security and Privacy (SP)*, 2018.
- [17] M. Mirman, T. Gehr, and M. Vechev, "Differentiable abstract interpretation for provably robust neural networks," in *International Conference on Machine Learning (ICML)*, 2018, pp. 3575–3583.
- [18] E. Wong and J. Z. Kolter, "Provable defenses against adversarial examples via the convex outer adversarial polytope," *International Conference on Machine Learning (ICML)*, 2018.
- [19] E. Wong, F. Schmidt, J. H. Metzen, and J. Z. Kolter, "Scaling provable adversarial defenses," *Advances in Neural Information Processing Systems (NIPS)*, 2018.
- [20] A. Madry, A. Makelov, L. Schmidt, D. Tsipras, and A. Vladu, "Towards deep learning models resistant to adversarial attacks," *International Conference on Learning Representations (ICLR)*, 2018.
- [21] A. Sinha, H. Namkoong, and J. Duchi, "Certifying some distributional robustness with principled adversarial training," *International Conference on Machine Learning (ICML)*, 2018.
- [22] K. Dvijotham, S. Gowal, R. Stanforth, R. Arandjelovic, B. O'Donoghue, J. Uesato, and P. Kohli, "Training verified learners with learned verifiers," *arXiv preprint arXiv:1805.10265*, 2018.
- [23] V. N. Vapnik, "An overview of statistical learning theory," *IEEE transactions on neural networks*, vol. 10, no. 5, pp. 988–999, 1999.
- [24] V. Vapnik, "Principles of risk minimization for learning theory," in *Advances in Neural Information Processing Systems (NIPS)*, 1992, pp. 831–838.
- [25] R. Huang, B. Xu, D. Schuurmans, and C. Szepesvári, "Learning with a strong adversary," *arXiv preprint arXiv:1511.03034*, 2015.
- [26] U. Shaham, Y. Yamada, and S. Negahban, "Understanding adversarial training: Increasing local stability of neural nets through robust optimization," *Neurocomputing*, 2018.
- [27] A. Kurakin, I. Goodfellow, and S. Bengio, "Adversarial machine learning at scale," *arXiv preprint arXiv:1611.01236*, 2016.
- [28] I. Goodfellow, J. Shlens, and C. Szegedy, "Explaining and harnessing adversarial examples," in *International Conference on Learning Representations (ICLR)*, 2015.
- [29] F. Tramèr, A. Kurakin, N. Papernot, I. Goodfellow, D. Boneh, and P. McDaniel, "Ensemble adversarial training: Attacks and defenses," *arXiv preprint arXiv:1705.07204*, 2017.
- [30] M. Ducoffe and F. Precioso, "Adversarial active learning for deep networks: a margin based approach," *arXiv preprint arXiv:1802.09841*, 2018.
- [31] A. Athalye, N. Carlini, and D. Wagner, "Obfuscated gradients give a false sense of security: Circumventing defenses to adversarial examples," *arXiv preprint arXiv:1802.00420*, 2018.
- [32] L. Schott, J. Rauber, M. Bethge, and W. Brende, "Towards the first adversarially robust neural network model on mnist," 2018. [Online]. Available: <https://arxiv.org/pdf/1805.09190.pdf>
- [33] K. Dvijotham, R. Stanforth, S. Gowal, T. Mann, and P. Kohli, "A dual approach to scalable verification of deep networks," *arXiv preprint arXiv:1803.06567*, 2018.
- [34] T.-W. Weng, H. Zhang, H. Chen, Z. Song, C.-J. Hsieh, D. Boning, I. S. Dhillon, and L. Daniel, "Towards fast computation of certified robustness for relu networks," *arXiv preprint arXiv:1804.09699*, 2018.
- [35] M. Anthony and P. L. Bartlett, *Neural network learning: Theoretical foundations*. Cambridge University Press, 2009.
- [36] Y. LeCun, L. Bottou, Y. Bengio, and P. Haffner, "Gradient-based learning applied to document recognition," *Proceedings of the IEEE*, vol. 86, no. 11, pp. 2278–2324, 1998.
- [37] A. Krizhevsky and G. Hinton, "Learning multiple layers of features from tiny images," Citeseer, Tech. Rep., 2009.
- [38] "Tiny ImageNet Visual Recognition Challenge," <https://tiny-imagenet.herokuapp.com/>.
- [39] D. P. Kingma and J. Ba, "Adam: A method for stochastic optimization," *International Conference on Learning Representations (ICLR)*, 2014.
- [40] H. Robbins and S. Monro, "A stochastic approximation method," in *Herbert Robbins Selected Papers*. Springer, 1985, pp. 102–109.
- [41] J. Kiefer, J. Wolfowitz *et al.*, "Stochastic estimation of the maximum of a regression function," *The Annals of Mathematical Statistics*, vol. 23, no. 3, pp. 462–466, 1952.
- [42] J. Deng, W. Dong, R. Socher, L.-J. Li, K. Li, and L. Fei-Fei, "ImageNet: A Large-Scale Hierarchical Image Database," in *CVPR09*, 2009.
- [43] O. Russakovsky, J. Deng, H. Su, J. Krause, S. Satheesh, S. Ma, Z. Huang, A. Karpathy, A. Khosla, M. Bernstein, A. C. Berg, and L. Fei-Fei, "ImageNet Large Scale Visual Recognition Challenge," *International Journal of Computer Vision (IJCV)*, vol. 115, no. 3, pp. 211–252, 2015.
- [44] J. Rauber, W. Brendel, and M. Bethge, "Foolbox v0. 8.0: A python toolbox to benchmark the robustness of machine learning models," *arXiv preprint arXiv:1707.04131*, 2017.
- [45] S. Gu and L. Rigazio, "Towards deep neural network architectures robust to adversarial examples," *arXiv preprint arXiv:1412.5068*, 2014.
- [46] N. Papernot and P. McDaniel, "Extending defensive distillation," *arXiv preprint arXiv:1705.05264*, 2017.
- [47] —, "Deep k-nearest neighbors: Towards confident, interpretable and robust deep learning," *arXiv preprint arXiv:1803.04765*, 2018.
- [48] J. Buckman, A. Roy, C. Raffel, and I. Goodfellow, "Thermometer encoding: One hot way to resist adversarial examples," 2018.
- [49] Y. Song, T. Kim, S. Nowozin, S. Ermon, and N. Kushman, "Pixeldefend: Leveraging generative models to understand and defend against adversarial examples," *arXiv preprint arXiv:1710.10766*, 2017.
- [50] C. Xie, J. Wang, Z. Zhang, Z. Ren, and A. Yuille, "Mitigating adversarial effects through randomization," *arXiv preprint arXiv:1711.01991*, 2017.
- [51] V. Zantedeschi, M.-I. Nicolae, and A. Rawat, "Efficient defenses against adversarial attacks," in *Proceedings of the 10th ACM Workshop on Artificial Intelligence and Security*. ACM, 2017, pp. 39–49.
- [52] N. Papernot, N. Carlini, I. Goodfellow, R. Feinman, F. Faghri, A. Matyasko, K. Hambardzumyan, Y.-L. Juang, A. Kurakin, R. Sheatsley *et al.*, "cleverhans v2. 0.0: an adversarial machine learning library," *arXiv preprint arXiv:1610.00768*, 2016.
- [53] G. F. Elsayed, S. Shankar, B. Cheung, N. Papernot, A. Kurakin, I. Goodfellow, and J. Sohl-Dickstein, "Adversarial examples that fool both human and computer vision," *arXiv preprint arXiv:1802.08195*, 2018.
- [54] N. Carlini and D. Wagner, "Adversarial examples are not easily detected: Bypassing ten detection methods," in *Proceedings of the 10th ACM Workshop on Artificial Intelligence and Security*. ACM, 2017, pp. 3–14.
- [55] B. Biggio, I. Corona, D. Maiorca, B. Nelson, N. Šrndić, P. Laskov, G. Giacinto, and F. Roli, "Evasion attacks against machine learning at test time," in *Joint European conference on machine learning and knowledge discovery in databases*. Springer, 2013, pp. 387–402.

- [56] X. Ma, B. Li, Y. Wang, S. M. Erfani, S. Wijewickrema, M. E. Houle, G. Schoenebeck, D. Song, and J. Bailey, "Characterizing adversarial subspaces using local intrinsic dimensionality," *arXiv preprint arXiv:1801.02613*, 2018.
- [57] C. Guo, M. Rana, M. Cisse, and L. van der Maaten, "Countering adversarial images using input transformations," *arXiv preprint arXiv:1711.00117*, 2017.
- [58] W. He, J. Wei, X. Chen, N. Carlini, and D. Song, "Adversarial example defenses: Ensembles of weak defenses are not strong," *arXiv preprint arXiv:1706.04701*, 2017.
- [59] A. Athalye and I. Sutskever, "Synthesizing robust adversarial examples," *International Conference on Machine Learning (ICML)*, 2018.
- [60] N. Carlini and D. Wagner, "Magnets and "efficient defenses against adversarial attacks" are not robust to adversarial examples," *arXiv preprint arXiv:1711.08478*, 2018.
- [61] K. Pei, Y. Cao, J. Yang, and S. Jana, "Deepxplore: Automated whitebox testing of deep learning systems," in *Proceedings of the 26th Symposium on Operating Systems Principles (SOSP)*. ACM, 2017, pp. 1–18.
- [62] Y. Tian, K. Pei, S. Jana, and B. Ray, "Deepest: Automated testing of deep-neural-network-driven autonomous cars," in *Proceedings of the 40th International Conference on Software Engineering*. ACM, 2018, pp. 303–314.
- [63] A. Lomuscio and L. Maganti, "An approach to reachability analysis for feed-forward relu neural networks," *arXiv preprint arXiv:1706.07351*, 2017.
- [64] X. Huang, M. Kwiatkowska, S. Wang, and M. Wu, "Safety verification of deep neural networks," in *International Conference on Computer Aided Verification (CAV)*. Springer, 2017, pp. 3–29.
- [65] R. Ehlers, "Formal verification of piece-wise linear feed-forward neural networks," *15th International Symposium on Automated Technology for Verification and Analysis*, 2017.
- [66] V. Tjeng, K. Xiao, and R. Tedrake, "Evaluating robustness of neural networks with mixed integer programming," *arXiv preprint arXiv:1711.07356*, 2017.
- [67] M. Fischetti and J. Jo, "Deep neural networks as 0-1 mixed integer linear programs: A feasibility study," *arXiv preprint arXiv:1712.06174*, 2017.
- [68] S. Dutta, S. Jha, S. Sankaranarayanan, and A. Tiwari, "Output range analysis for deep feedforward neural networks," in *NASA Formal Methods Symposium*. Springer, 2018, pp. 121–138.
- [69] A. Raghunathan, J. Steinhardt, and P. Liang, "Certified defenses against adversarial examples," *International Conference on Learning Representations (ICLR)*, 2018.
- [70] T.-W. Weng, H. Zhang, P.-Y. Chen, J. Yi, D. Su, Y. Gao, C.-J. Hsieh, and L. Daniel, "Evaluating the robustness of neural networks: An extreme value theory approach," *International Conference on Learning Representations (ICLR)*, 2018.
- [71] S. Zagoruyko and N. Komodakis, "Wide residual networks," *British Machine Vision Conference (BMVC)*, 2016.

APPENDIX

A. Memory Usage

MixTrain is able to significantly cut down memory usage during robust training compared to state-of-the-art verifiable robust training [19]. This allows MixTrain to run on limited GPU resources. Here, in Table X, we summarize the GPU memory required for regular training, MixTrain and Wong et al. [19] for each network. ϵ is set to 0.3 for MNIST dataset and 0.0348 for CIFAR dataset. For Wong et al.'s method [19], even after applying 50 random projection proposed in [19] to cut down memory usage, it still needs 4 GeForce GTX 1080 Ti GPUs to train large networks with batch size 50. In contrast, MixTrain requires only 1 GPU to train these networks. Overall, MixTrain, on average, uses $10\times$ less GPU memory than Wong et al.'s method. Note that, as shown in Table IV and V, MixTrain further provides similar or even better accuracy and robustness in less training time compared to Wong et al.'s method [19].

Network	Memory Usage (MB)		
	Baseline	MixTrain	Wong et al. [19]
MNIST_Small	533	837	5,474
MNIST_Large	629	6,383	32,626
CIFAR_Small	553	869	17,960
CIFAR_Large	621	5,335	39,840
CIFAR_Resnet	589	3,475	3,7784

TABLE X: The GPU memory usage required to train different networks by using MixTrain compared to regular training (Baseline) and state-of-the-art verifiable robust training method [19]. ϵ is 0.3 for MNIST dataset and 0.0348 for CIFAR dataset.

B. Network Architectures

Below we describe the architectures of the 6 different networks we used for our evaluation. We use $Conv_s C \times W \times H$ to denote a convolutional layer that has C channels with kernel size (W, H) and stride s . $FC n$ denotes a fully connected layer that contains n hidden nodes and $Res C \times W \times H$ denotes the residual modules defined in [71] that has C output channels with kernel size (W, H) . Each residual module contains two convolutional layers each with ReLU and one skip connection from input.

MNIST_FC1. Small fully connected network for MNIST:

$$x \rightarrow FC\ 512 \rightarrow ReLU \rightarrow FC\ 512 \rightarrow ReLU \rightarrow f_{\theta}(x)$$

MNIST_FC2. Large fully connected network for MNIST:

$$\begin{aligned} x &\rightarrow FC\ 2048 \rightarrow ReLU \rightarrow FC\ 2048 \rightarrow ReLU \\ &\rightarrow FC\ 2048 \rightarrow ReLU \rightarrow FC\ 2048 \rightarrow ReLU \\ &\rightarrow FC\ 2048 \rightarrow ReLU \rightarrow f_{\theta}(x) \end{aligned}$$

MNIST_Small & CIFAR_Small. Small convolutional network for MNIST and CIFAR used in [18]:

$$\begin{aligned} x &\rightarrow Conv_2 16 \times 4 \times 4 \rightarrow ReLU \rightarrow Conv_2 32 \times 4 \times 4 \\ &\rightarrow ReLU \rightarrow FC\ 100 \rightarrow ReLU \rightarrow f_{\theta}(x) \end{aligned}$$

MNIST_Large & CIFAR_Large. Large convolutional networks that are the extensions of small convolutional ones:

$$\begin{aligned} x &\rightarrow Conv_1 32 \times 3 \times 3 \rightarrow ReLU \rightarrow Conv_2 32 \times 4 \times 4 \\ &\rightarrow ReLU \rightarrow Conv_1 64 \times 3 \times 3 \rightarrow ReLU \\ &\rightarrow Conv_2 64 \times 4 \times 4 \rightarrow ReLU \rightarrow FC\ 512 \\ &\rightarrow ReLU \rightarrow FC\ 512 \rightarrow ReLU \rightarrow f_{\theta}(x) \end{aligned}$$

CIFAR_Resnet. The residual networks use the same in [71]:

$$\begin{aligned} x &\rightarrow Conv_1 16 \times 3 \times 3 \rightarrow ReLU \rightarrow Res\ 16 \times 3 \times 3 \\ &\rightarrow Res\ 32 \times 3 \times 3 \rightarrow Res\ 32 \times 3 \times 3 \\ &\rightarrow Res\ 64 \times 3 \times 3 \rightarrow Res\ 64 \times 3 \times 3 \\ &\rightarrow FC\ 1000 \rightarrow ReLU \rightarrow f_{\theta}(x) \end{aligned}$$

ImageNet_Resnet. The residual networks use the same structure as in [71] for Imagenet-200 dataset [38]. To improve training efficiency, we crop the original shape of image $3 \times 64 \times 64$ to $3 \times 32 \times 32$. Such data augmentation help to speed up the the training procedure without sacrificing too much accuracy.

$$\begin{aligned} x &\rightarrow Conv_1 16 \times 3 \times 3 \rightarrow ReLU \rightarrow Res\ 16 \times 3 \times 3 \\ &\rightarrow Res\ 32 \times 3 \times 3 \rightarrow Res\ 32 \times 3 \times 3 \\ &\rightarrow Res\ 64 \times 3 \times 3 \rightarrow Res\ 64 \times 3 \times 3 \\ &\rightarrow FC\ 1000 \rightarrow ReLU \rightarrow f_{\theta}(x) \end{aligned}$$